Journal of Materials Chemistry A

p-Type BP Nanosheet Photocatalyst with AQE of 3.9% in the Absence of a Noble Metal Cocatalyst: Investigation and Elucidation of Photophysical Properties

Journal:	*Journal of Materials Chemistry A*
Manuscript ID	TA-COM-07-2018-007034.R1
Article Type:	Communication
Date Submitted by the Author:	17-Aug-2018

Complete List of Authors:	Rahman, Mohammad; University of Texas at Austin, Department of Chemical Engineering Batmunkh, Munkhbayar; University of Queensland Faculty of Humanities and Social Sciences Bat-Erdene, Munkhjargal; Flinders University, School of Chemical and Physical Sciences Shapter, Joseph; Flinders University Mullins, Charles; University of Texas at Austin, Department of Chemical Engineering

Journal Name

COMMUNICATION

p-Type BP Nanosheet Photocatalyst with AQE of 3.9% in the Absence of a Noble Metal Cocatalyst: Investigation and Elucidation of Photophysical Properties

Received 00th January 20xx,
Accepted 00th January 20xx

DOI: 10.1039/x0xx00000x

www.rsc.org/

Mohammad Z. Rahman[a, c], Munkhbayar Batmunkh[b], Munkhjargal Bat-Erdene[b], Joseph G. Shapter[b]*, and Charles B. Mullins[a]*

While stability, significantly poor apparent quantum efficiency (AQE < 0.5%) and over dependence on noble metal cocatalysts is a long standing probelem, here, we report, for the first time, microwave-exfoliated p-type few-layer black phosphorous (BP-nanosheets) as a stable photocatalyst for hydrogen production without any supporting noble metal co-catalyst. This few layer BP has shown a record high apparent quantum efficiency (AQE) of ~ 4 % at 420 nm under visible light irradiation. This unprecedented AQE stems from a low level of material oxidation that impedes the degradation of BP under ambient conditions, strong absorption of photons at the surface, and a conduction band edge position that favorably facilitates the proton reduction reaction. These BP-nanosheets have also shown superior photocatalytic performance compared to the known cohort of metal-free photocatalysts such as graphitic carbon nitride, carbon dots, and red-P under identical experimental conditions. An understanding of the photo-physicochemical reasons that drive this chemistry is elucidated along with results obtained from physicochemical characterization and finite difference time domain simulations.

The combustion of fossil fuels is the primary cause of global warming causing pervasive and lasting damage to the earth's climate and ecosystems.[1] Additionally, the fast depletion of fossil fuel sources creates a daunting threat regarding the scarcity and reliability of energy sources in the foreseeable future.[2] To ensure a sustainable energy supply and to mitigate the potentially catastrophic effects of climate change, solar energy needs to be harvested to produce useful energy.[3] Photocatalytic hydrogen production from water in this regard is a promising approach for converting solar energy into readily usable chemical energy.[4] Importantly, hydrogen can be stored directly, used on demand, and it burns cleanly back to water without production of any CO_2.[5, 6]

The cornerstone of any photocatalytic process is a light absorbing material known as photocatalyst. The materials synthesized as photocatalysts in the intervening four decades can be conveniently categorized into metal-based and metal-free photocatalysts. Although most research has been devoted to developing metal-based photocatalysts, the recent synthesis of metal-free photocatalysts has gained some momentum, especially considering some of the serious drawbacks of metal-based photocatalysts, particularly their corrosiveness and toxicity to humans.[7-9] A key breakthrough was metal-free graphitic carbon nitride.[10, 11] This is a non-toxic, highly stable material in both acidic and alkaline solution, and is independent of noble metal cocatalysts for hydrogen evolution. Other metal-free photocatalysts include elemental red-phosphorous (red-P), alpha-Sulfur (α-S_8), and boron. [12-14] In a quest for new metal-free photocatalysts, recently, black phosphorous (BP) has been explored with regard to hydrogen production. [15-17] Interest in BP started because it can be exfoliated into 2D few-layer to monolayer sheets (known as phosphorene [18-20]) that have shown a tunable bandgap and anisotropic properties. It is currently being studied for applications in transistors, optoelectronics, batteries, gas storage and solar cells.[21-24]

Theoretically, few-layer BP (*alias* phosphorene) has exhibited some properties that are highly desirable in photocatalysis applications. These include (i) quantum confinement in the direction perpendicular to the 2D plane, which results in noble electronic and optical properties; (ii) natural surface passivation without any dangling bonds (a suppressed carrier recombination is expected); (iii) no lattice mismatch issues for constructing vertical heterostructures with other 2D materials; (iv) large lateral size with ultra-high specific surface area and high ratios of exposed surface atoms; and, (v) a strong interaction with light. [25-29] Indeed, Sa et al. and Hu et al. theoretically studied the photocatalytic activities of phosphorene.[30, 31] We have recently reviewed the

[a] *John J. Mcketta Department of Chemical Engineering and Department of Chemistry, The University of Texas at Austin, TX 78712, USA.*
[b] *Australian Institute of Bioengineering and Nanotechnology (AIBN), University of Queensland, St. Lucia, Queensland 4072, Australia*
[c] *School of Chemical Engineering, The University of Adelaide,, SA 5005, Australia*
Corresponding author e-mail: mullins@che.utexas.edu; j.shapter@uq.edu.au
Electronic Supplementary Information (ESI) available: [details of any supplementary information available should be included here]. See DOI: 10.1039/x0xx00000x

fundamental properties to assess its suitability as a water-splitting photocatalyst. [28]

The favourable properties of few-layer BP have inspired researchers to investigate its practical suitability as a photocatalyst. Zhu et al. demonstrated lithium intercalated BP-nanosheets for photocatalytic hydrogen evolution with an apparent quantum efficiency (AQE) of 0.47 % at 420 nm in the presence of sacrificial electron donors (SED).[15] Recently, Tian et al. reported wet-chemical synthesis of few-layer BP nanosheets for photocatalytic hydrogen production with a hydrogen production rate of ~0.36 µmol h^{-1} at 420 nm.[16] When incorporated with a high loading of Pt (20 wt. %), it showed a hydrogen production rate of ~11.1 µmol h^{-1} at 420 nm with an AQE of ~4%. Although avoiding the use of Pt for low-cost hydrogen production is desirable, the use of Pt here appears to be unavoidable for the purpose of charge transfer and catalysis, which leads to enhanced hydrogen evolution. However, an increased AQE with Pt as a cocatalyst doesn't really reflect the increased intrinsic catalytic activity of BP, but rather seems to indicate that BP is somewhat inactive without Pt. These findings clearly indicate that more research needs to be carried out to enhance the quantum yield of hydrogen production on BP-nanosheets in the absence of Pt (and other precious metals) for low-cost and sustainable photocatalytic hydrogen production.

Here we report microwave exfoliated few-layer thick BP as a stable hydrogen evolution photocatalyst. This few-layer thick BP exhibits a record high hydrogen production rate of 17.9 µmol h^{-1} with an AQE of ~4 % at 420 nm under visible light irradiation in the absence of a Pt cocatalyst. Our investigation shows that this AQE for BP is also higher than that of carbon nitride, carbon dots, and red-P under identical photocatalytic conditions (data not shown here). To understand the catalyst activities, we have probed the relevant attributes of few-layer BP through photo-physicochemical characterization and finite difference time domain (FDTD) simulations.

The synthesis process significantly influences the stability of few-layer BP at ambient conditions.[32-34] The synthesis of few-layer BP using the more common techniques, such as, mechanical cleavage and liquid–exfoliation, has proven to be unstable.[18, 24, 32, 35] BP-nanosheets synthesized by Ball-milling with LiOH were shown to be stable, however, this process can create violent sparking, and unless removed completely, the presence of Li can induce undesired charging effects.[15] Contrarily, the few-layer BP in our experiments was produced using a microwave-assisted exfoliation technique (*see* Supporting Information for the detailed synthesis procedure). Briefly, when MW irradiation is applied to the sample, van der Waals interactions between the bulk BP flakes start weakening and further exfoliates layer by layer in the appropriate solvent.[36] This few-layer BP can be solution processed and shows low oxidation levels in ambient conditions. Moreover, the microwave assisted exfoliation technique can produce high quality BP nanosheets in less than 12 min.

We have investigated the morphology of our synthesized BP nanosheets using Atomic Force Microscopy (AFM) Transmission Electron Microscopy (TEM) and X-ray Diffraction (XRD). The AFM image shows a mix of large and small area nanoflakes (Figure S1). The height profile measurements shows that the thickness of these flakes can vary by up to 15 nm (Figure S1) with a lateral size up to 5 µm indicating dispersed phosphorene nanoflakes of single to multilayers. Raman spectroscopy and spectral bandgap calculations (discussed in the following paragraphs) indicate that most of the flakes are bi-layers. The AFM results are supported by the TEM image (Figure 1a) which clearly shows dispersed nanosheets of various sizes. XRD patterns (Figure S2) show characteristic peaks that are identical to previous reports. [15] The sharp peaks support a highly crystalline structure. A high-resolution TEM image (Figure S3) also shows that these nanosheets are crystalline with defined atomic fringes. Therefore, the material produces ordered diffraction spots in selected area diffraction (SAED) measurements as is shown in the inset of Figure 1c. These results are consistent with previously published results.[16, 32, 37]

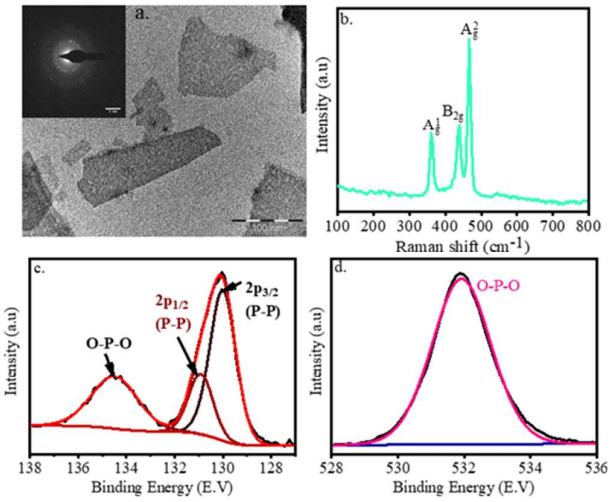

Figure 1. a) TEM image, scale bar 100 nm. Inset is the SAED pattern, b) Raman spectra, c). Deconvoluted P2p XPS spectra, and d) Deconvoluted O1s XPS spectra of BP-nanosheets.

We have probed the chemical nature and structural stability of few-layer BP using confocal Raman spectroscopy and X-ray photoelectron spectroscopy (XPS). The Raman spectrum exhibited characteristic A_g^1, B_{2g}, and A_g^2 phonon modes at ~362, ~440, and ~467 cm^{-1}, respectively, Figure 1b.[38] These are the signature phonon modes that are usually observed in BP nanosheets. The origin of the A_g^1 mode is due to the out-of-plane vibrations of phosphorus atoms along the c-axis, and the B_{2g} and A_g^2 modes originate due to the in-plane vibrations of phosphorus atoms along the b-axis (armchair) and a-axis (zigzag), respectively.[39] The intensity of the A_g^2 mode is disprotionately high with respect to that of the A_g^1 and B_{2g} modes, indicating that the BP-flakes are mainly bi-layers. The same result was observed by Favron et al.[32] There was no peak observed at ~ 400 cm^{-1} which would have signified that the BP nanosheets were not partially oxidized.[32, 40] Additionally, another signature of low-oxidation levels, according to Fevron et al., is the absence of broad features in

the region under B_{2g} and A_g^2, and an intensity ratio of A_g^1 / A_g^2 > 0.2.[24, 28] These results show that these microwave-assisted few-layer BP nanosheets are structurally highly robust against ambient oxidation. This is also corroborated from the deconvoluted P2p and O1s XPS spectra. Background corrected (using the Shirley algorithm) and deconvoluted (using a Gaussian–Lorentzian function) P2p XPS

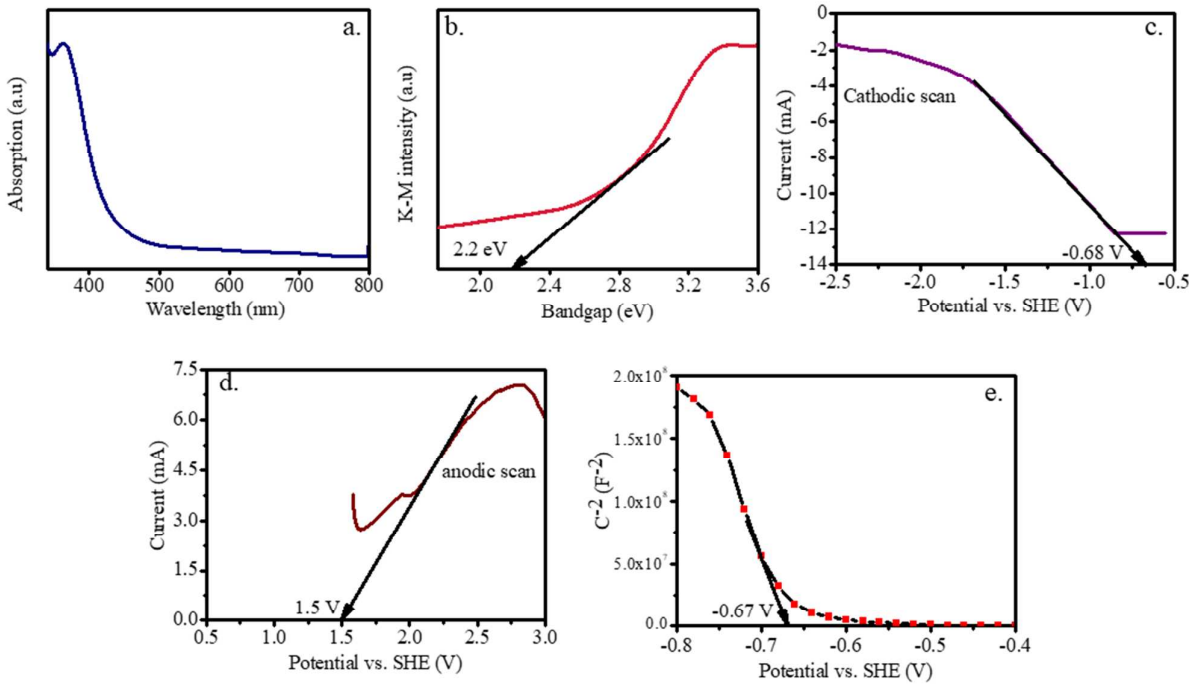

Figure 2. a) UV-Vis spectra of BP-nanosheets, b) K-M plot for bandgap calculation using the formula $(h\nu\alpha)^n$. BP is considered as a direct bandgap semiconductor, and therefore n = 0.5, c) Cathodic scan for determining CBM position, d) Anodic scan for determining VBM position, and e) Mott-Schottky plot for determining CBM position.

spectra shows $P2p_{3/2}$ and $P2p_{1/2}$ states for the P-P bond at ~ 130 eV and 130.5 eV, and a bridge bonded P-O-P structure at ~134 eV, respectively (Figure 1c).[15, 39] The presence of P-O-P bonds indicates the inevitable adsorption of oxygen which was previously shown as beneficial for photocatalytic hydrogen evolution. Analysis of the chemical composition shows that only a small amount of oxygen is present in the BP nanosheets (*see* Figure S4). The absence of any P=O (dangling bonds) and P_2O_5 peaks in the deconvoluted O1s XPS spectra (Figure 1d) however indicate that the BP nanosheets are not oxidized. [15, 16, 39]

We have also studied the optical absorption properties and suitability of BP nanosheets as a hydrogen evolution (HER) photocatalyst using diffuse reflectance spectroscopy and electrochemical characterization. Figure 2a, b shows the UV-Vis spectra and a corresponding Kubelka-Munk (K-M) plot, respectively. A bandgap of ~2.2 eV has been extrapolated from the K-M plot. This UV-Vis spectra has shown good agreement with theoretical absorption spectra (see Figure S5). The conduction band minimum (CBM) and valance band maximum (VBM) of the BP nanosheets were determined using linear potential scans.[41, 42] In a linear potential scan, the creation of accumulation/inversion layers above the CBM potential and below the VBM potential, respectively, can lead to the emergence of cathodic/anodic current.[41] The extrapolated CBM and VBM values from cathodic and anodic scans are −0.68 and 1.5 V vs SHE (standard hydrogen electrode), respectively (Figure 2c, d). This results in a bandgap equal to 2.18 eV which is in a good agreement with that obtained from optical absorption spectra. We further checked and confirmed the CBM position from impedance spectroscopy in which Mott–Schottky (M–S) plots were acquired at an AC frequency of 1 kHz. The negative slope in the M-S plot indicates that our BP nanosheet sample is a p-type semiconductor (Figure 2e). As is shown in Figure 3a, the CB position (- 0.68 V vs. SHE) is more negative than the proton reduction potential ($H+/H_2$ = 0.0 V vs SHE), and therefore provides sufficient electronic potential to meet the thermodynamic requirements of the HER.

The as-prepared BP nanosheets were then subjected to a photocatalytic hydrogen production test. Despite suitable CB and VB positions for water-splitting, we only observed hydrogen production of 1.3 µmol h^{-1} from pure water while there was zero oxygen evolution (Figure 3b). We suspect that the quantity of evolved oxygen is much lower than the detection limit of our Gas Chromatograph. Tian et al. also observed only hydrogen evolution when photocatalytic testing was performed in pure water.[16] We then focused on hydrogen evolution by suppressing oxygen evolution. We used triethanolamine as a sacrificial agent to scavenge holes to suppress the oxygen evolution. The TEOA becomes oxidized by the holes in the photocatalytic hydrogen production process. BP nanosheets can produce hydrogen from water-triethanolamine (10 vol. %) at a rate of 17.9 µmol h^{-1} under visible light irradiation (300 W Xe lamp with 420 nm cut-off

filter) without any co-catalyst (Figure 3b). The calculated apparent quantum efficiency (AQE) is 3.9 % at 420 nm. To the best of our knowledge, this is the highest AQE demonstrated to date for hydrogen production on standalone black phosphorous derivatives as a photocatalyst (*see* the Table S1) in the absence of a cocatalyst.

We also evaluated the hydrogen production on metal-free carbon nitride (CN), carbon dots (CD) and red-P (RP) under identical photocatalytic experimental conditions for comparison. The measured hydrogen production rates were 5.5, 0.0, and 1.3 μmol h^{-1} for CN, CD and RP, respectively. Clearly, microwave exfoliated BP nanosheets exhibit superior performance compared to that of CN, CD and RP. We then extended our research to assess the cocatalyst activity of BP-nanosheets when incorporated with CN, CD and RP (*see* the Supplementary Notes 1, and associated supplementary figures for details). Interestingly, BP-nanosheets showed comparable performance to that of noble metal Pt- indicating the suitability

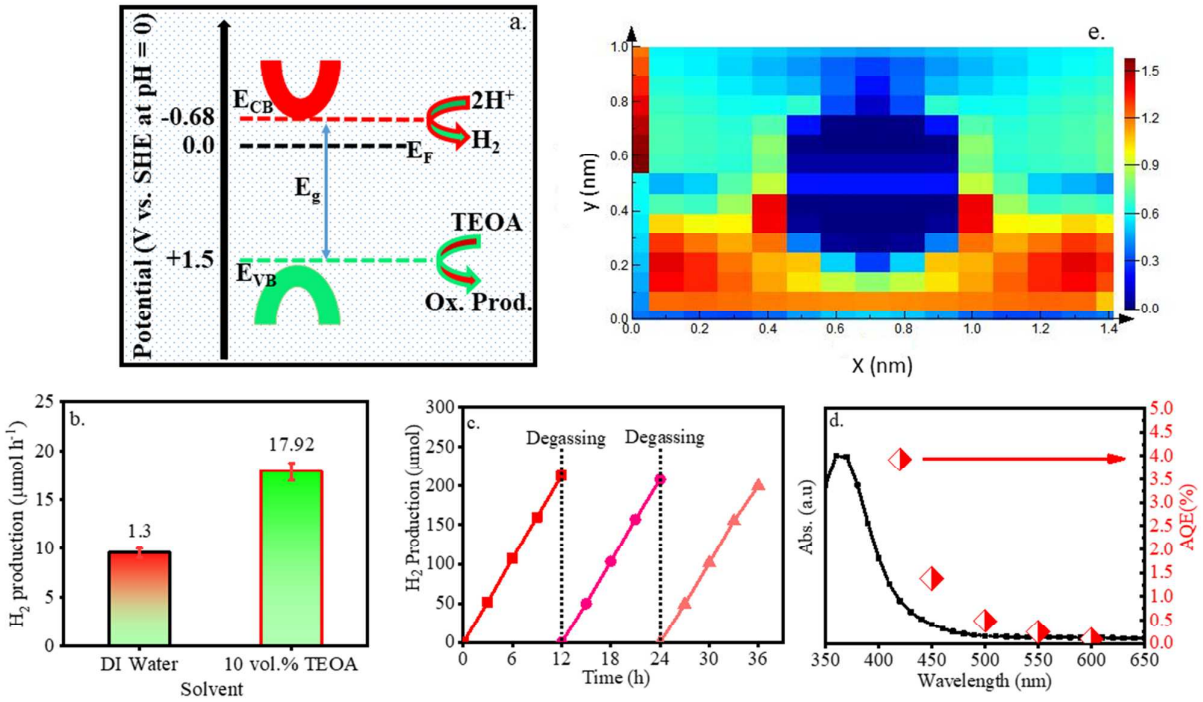

Figure 3. a) Hypothetical schematic presentation of energy level of conduction band (E_{CB}) and valence band (E_{VB}) with respect to Fermi energy level (E_F), showing BP-nanosheets have sufficient electronic potential to drive HER, b) Rate of hydrogen production DI water and water-triethanolamine solution, respectively under visible light (420 nm) irradiation, c) Cyclic hydrogen production under visible light (420 nm) irradiation for probing photocatalytic stability, d) Wavelength dependent hydrogen production, and e) Understanding the probabilistic distribution of charge carriers through FDTD simulations.

of BP-nanosheets to be used as Pt substituted metal-free cocatalyst. It is strongly desirable to avoid Pt for scalable and low-cost hydrogen production, therefore this is a highly interesting result for shifting the paradigm from a Pt to a non-Pt era.

We also evaluated the photocatalytic stability of few-layer BP. As is shown in Figure 3c, we didn't observe any noticeable degradation in cyclic hydrogen production indicating the photocatalytic stability of BP-nanosheets. We have probed the structural stability by measuring the XRD and XPS spectra of the sample before and after photocatalytic reactions. BP nanosheets retain the identical spectra before and after photocatalytic reactions (*see* Figure S6), and therefore confirm the structural stability. To confirm that hydrogen is evolved only via photocatalytic processes, we carried out wavelength dependent hydrogen production. We observed that the wavelength dependent hydrogen production roughly followed the absorption spectra (*see* Figure 3d). There was no hydrogen production in the dark. Although BP-nanosheets showed a broad absorption spectra that extended to the near infrared (NIR), we didn't detect any hydrogen production beyond 550 nm. This could plausibly be because: (i) the electrons that were generated by excitation of photons having wavelengths higher than 550 nm might not have sufficient energy to reach the conduction band or undergo rapid trapping in deep/shallow traps states, and/or (ii) forbidden π-nπ* transition of electrons from the valence band to the conduction band.[43] However, more research is needed to unveil the actual reasons.

We extended our investigations to determine the statistical charge carrier generation and the accessibility of charge carriers to the surface of the BP-nanosheets for carrying out the proton reduction reaction. Gradual decreases in hydrogen production with increasing wavelength can be correlated to asymmetric/non-homogeneous charge carrier generation in the material as well as the corresponding availability of electrons that are active for the proton reduction reaction. To probe this possibility, the identification of the catalytically active sites considering photogeneration is necessary. However, there have been no such prior studies for BP-nanosheets. To assess this, we carried out finite difference

time domain (FDTD) simulations.[44, 45] When few-layer BP is subjected to irradiation from the UV-VIS to NIR, the probabilistic distribution pattern of the generation of charge carriers within a given area of the nanosheets will provide an idea of the active site locations for catalytic reactions.

In the FDTD simulations, a BP-nanosheet was subjected to illumination from a continuum electro-magnetic light source to acquire the absorption spectra that matches the experimental data (Figure S3). The lateral sizes of the modelled nanosheets was set to 1 – 1.4 nm. The simulated distribution of photogenerated charge carriers is shown in Figure 3e. From the simulation results, the rate of generation is found to be inversely proportional to the distance from the surface to the bulk. We have noticed a strong absorption of photon energy on the surface, and therefore generation of charge carriers is more significant at a distance up to 0.4 nm from the surface. Above 0.4 nm, this generation rate gradually decreased and eventually reached zero at some points. This indicates that the photogeneration of charge carriers in BP-nanosheets is inhomogeneous, and the probability of accommodating catalytic active sites with electrons therefore is high within a distance of 0 – 0.4 nm from the surface. It also means that vectorial transfer of electrons requires travel of a distance of about 0.4 nm to reach the surface which seems very promising for enhanced proton reduction. Despite the short migration distance for electrons, a low rate of hydrogen evolution could presumably be due to high surface and bulk recombination of electron-hole pairs, and/or resistive pathways for transferring electrons to the surface.[43, 46, 47]

Conclusions

In conclusion, microwave exfoliated p-type few-layer BP (BP-nanosheets) has been demonstrated as a photocatalyst for hydrogen production. The physicochemical characterizations and FDTD simulations revealed some of the intriguing properties of these nanosheets such as a low-oxidation level that prevents degradation, suitable bandgap and band edges, high surface electrons concentrations, and minimum distance for electron transfer from bulk to catalytic sites. All these properties cumulatively resulted in a record high hydrogen production with an AQE of ~3.9 % from 10 vol. % water-triethanolamine at 420 nm under visible light irradiation without a noble-metal cocatalyst. This result therefore opens a new avenue of study for hydrogen production independent of noble-metal cocatalysts. BP-nanosheets can also be combined with an oxygen evolution photocatalyst to realize overall water-splitting. For further increases in hydrogen production, studies are needed to understand the percolation of charge carriers, and the complex interaction of recombination, trapping and transport of charge carriers from the point of generation to the surface.

Conflicts of interest

There are no conflicts to declare.

Acknowledgements

The use of South Australian nodes of the Australian Microscopy & Microanalysis Research Facility (AMMRF) and Australian National Fabrication Facility (ANFF) at Flinders University is acknowledged. The authors would also like to thank Dr. Christopher T. Gibson of the College of Science and Engineering at Flinders University for his help with AFM characterization. CBM acknowledges the Welch Foundation (Grant no. 1436) and the United States Department of Energy, Basic Energy Sciences (Grant no. DE-FG02-09ER16119) for their generous support.

References

1. S. J. Davis, K. Caldeira and H. D. Matthews, *Science*, 2010, **329**, 1330.
2. M. Ball, M. Ball and M. Wietschel, *Hydrogen Economy,* **2009**, 46-114.
3. T. A. Faunce, W. Lubitz, A. W. Rutherford, D. MacFarlane, G. F. Moore, P. Yang, D. G. Nocera, T. A. Moore, D. H. Gregory, S. Fukuzumi, K. B. Yoon, F. A. Armstrong, M. R. Wasielewski and S. Styring, *Energy Environ. Sci.*, 2013, **6**, 695.
4. M. Z. Rahman, Y. Tang and P. Kwong, *Appl. Phys. Lett.*, 2018, **112**, 253902.
5. A. J. Esswein and D. G. Nocera, *Chem. Rev.*, 2007, **107**, 4022-4047.
6. N. S. Lewis and D. G. Nocera, *Proc. Natl Acad. Sci. USA*, 2006, **103**, 15729-15735.
7. A. Fujishima and K. Honda, *Nature*, 1972, **238**, 37-38.
8. H. Kazuhito, I. Hiroshi and F. Akira, *Jap. J. Appl. Phys.*, 2005, **44**, 8269.
9. A. Kudo and Y. Miseki, *Chem. Soc. Rev.*, 2009, **38**, 253-278.
10. X. Wang, K. Maeda, A. Thomas, K. Takanabe, G. Xin, J. M. Carlsson, K. Domen and M. Antonietti, *Nat. Mater.*, 2009, **8**, 76-80.
11. M. Z. Rahman, K. Davey and S.-Z. Qiao, *J. Mater. Chem. A*, 2018, **6**, 1305-1322.
12. F. Wang, W. K. H. Ng, J. C. Yu, H. Zhu, C. Li, L. Zhang, Z. Liu and Q. Li, *Appl. Catal. B: Environ.*, 2012, **111-112**, 409-414.
13. G. Liu, P. Niu, L. Yin and H.-M. Cheng, *J. Am. Chem. Soc.*, 2012, **134**, 9070-9073.
14. G. Liu, L.-C. Yin, P. Niu, W. Jiao and H.-M. Cheng, *Angew. Chem. Int. Ed.*, 2013, **52**, 6242-6245.
15. X. Zhu, T. Zhang, Z. Sun, H. Chen, J. Guan, X. Chen, H. Ji, P. Du and S. Yang, *Adv. Mater.*, 2017, **29**, 1605776.
16. B. Tian, B. Tian, B. Smith, M. C. Scott, Q. Lei, R. Hua, Y. Tian and Y. Liu, *Proc. Natl. Acad. Sci. USA*, 2018, **115**, 4345-4350.
17. M. Zhu, Y. Osakada, S. Kim, M. Fujitsuka and T. Majima, *Appl. Catal. B: Environ.*, 2017, **217**, 285-292.
18. H. Liu, A. T. Neal, Z. Zhu, Z. Luo, X. Xu, D. Tománek and P. D. Ye, *ACS Nano*, 2014, **8**, 4033-4041.
19. L. Li, Y. Yu, G. J. Ye, Q. Ge, X. Ou, H. Wu, D. Feng, X. H. Chen and Y. Zhang, *Nat. Nanotechnol.*, 2014, **9**, 372-377.
20. T. Nilges, *Proc. Natl. Acad. Sci. USA*, 2018, **115**, 4311-4313.

21. L. Kou, C. Chen and S. C. Smith, *J. Phys. Chem. Lett.*, 2015, **5**, 2675.
22. L. Kou, T. Frauenheim and C. Chen, *J. Phys. Chem. Lett.*, 2014, **5**, 2675-2681.
23. M. Batmunkh, M. Bat-Erdene and J. G. Shapter, *Adv. Energy Mater.*, 2018, **8**, 1701832.
24. H. Liu, Y. Du, Y. Deng and P. D. Ye, *Chem. Soc. Rev.*, 2015, **44**, 2732-2743.
25. J. Low, S. Cao, J. Yu and S. Wageh, *Chem. Commun.*, 2014, **50**, 10768-10777.
26. K. S. Novoselov, D. Jiang, F. Schedin, T. J. Booth, V. V. Khotkevich, S. V. Morozov and A. K. Geim, *Proc. Natl. Acad. Sci. USA*, 2005, **102**, 10451-10453.
27. F. Xia, H. Wang, D. Xiao, M. Dubey and A. Ramasubramaniam, *Nat. Photon.*, 2014, **8**, 899-907.
28. M. Z. Rahman, C. W. Kwong, K. Davey and S. Z. Qiao, *Energy Environ. Sci.*, 2016, **9**, 709-728.
29. Y. Jing, X. Zhang and Z. Zhou, *Wiley Interdisciplinary Rev.: Comput. Mol. Sci.*, 2016, **6**, 5-19.
30. B. Sa, Y.-L. Li, J. Qi, R. Ahuja and Z. Sun, *J. Phys. Chem. C*, 2014, **118**, 26560-26568.
31. W. Hu, L. Lin, R. Zhang, C. Yang and J. Yang, *.J Am. Chem. Soc.*, 2017, **139**,15429–15436.
32. A. Favron, E. Gaufres, F. Fossard, A. L. Phaneuf-L'Heureux, N. Y. Tang, P. L. Levesque, A. Loiseau, R. Leonelli, S. Francoeur and R. Martel, *Nat. Mater.*, 2015, **14**, 826-832.
33. Y. Huang, J. Qiao, K. He, S. Bliznakov, E. Sutter, X. Chen, D. Luo, F. Meng, D. Su, J. Decker, W. Ji, R. S. Ruoff and P. Sutter, *Chem. Mater.*, 2016, **28**, 8330-8339.
34. K. L. Kuntz, R. A. Wells, J. Hu, T. Yang, B. Dong, H. Guo, A. H. Woomer, D. L. Druffel, A. Alabanza, D. Tomanek and S. C. Warren, *ACS Appl. Mater. Interfaces*, 2017, **9**, 9126-9135.
35. J. R. Brent, N. Savjani, E. A. Lewis, S. J. Haigh, D. J. Lewis and P. O'Brien, *Chem. Commun.*, 2014, **50**, 13338-13341.
36. M. Bat-Erdene, M. Batmunkh, C. J. Shearer, S. A. Tawfik, M. J. Ford, L. Yu, A. J. Sibley, A. D. Slattery, J. S. Quinton, C. T. Gibson and J. G. Shapter, *Small Meth.*, 2017, **1**, 1700260.
37. V. Eswaraiah, Q. Zeng, Y. Long and Z. Liu, *Small*, 2016, **12**, 3480-3502.
38. F. Xia, H. Wang and Y. Jia, *Nat. Commun.*, 2014, **5**, 4458.
39. S. Walia, S. Balendhran, T. Ahmed, M. Singh, C. El-Badawi, M. D. Brennan, P. Weerathunge, M. N. Karim, F. Rahman, A. Rassell, J. Duckworth, R. Ramanathan, G. E. Collis, C. J. Lobo, M. Toth, J. C. Kotsakidis, B. Weber, M. Fuhrer, J. M. Dominguez-Vera, M. J. S. Spencer, I. Aharonovich, S. Sriram, M. Bhaskaran and V. Bansal, *Adv. Mater.*, 2017, 29, 1700152.
40. Q. Zhou, Q. Chen, Y. Tong and J. Wang, *Angew. Chem. Int. Ed.*, 2016, **55**, 11437-11441.
41. T.-F. Yeh, C.-Y. Teng, S.-J. Chen and H. Teng, *Adv. Mater.*, 2014, **26**, 3297-3303.
42. M. Rahman, K. Davey and S.-Z. Qiao, *Small*, 2017, **13**, 1700376.
43. M. Z. Rahman, P. C. Tapping, T. W. Kee, R. Smernik, N. Spooner, J. Moffatt, Y. Tang, K. Davey and S.-Z. Qiao, *Adv. Funct. Mater.*, 2017, **27**, 1702384.
44. M. Z. Rahman, J. Moffatt and N. A. Spooner, *Mater. Horiz.*, 2018, **5**, 553.
45. Y. Li, Z. Ruan, Y. He, J. Li, K. Li, Y. Jiang, X. Xu, Y. Yuan and K. Lin, *Appl. Catal. B: Environ.*, 2018, **236**, 64-75.
46. M. Rahman, K. Davey and S. Z. Qiao, *Small*, 2017, **13**, 1700376.
47. M. Z. Rahman, *Renewable Sustainable Energy Rev.*, 2014, **30**, 734-742.

TOC

Title: p-Type BP Nanosheet Photocatalyst with AQE of 3.9% in the Absence of a Noble Metal Cocatalyst: Investigation and Elucidation of Photophysical Properties

Authors: M*ohammad* Z. Rahman, M*unkhbayar* Batmunkh, M*unkhjargal Bat-Erdene*, J*oseph G.* Shapter, *and Charles* B. Mullins

Keywords: Black phosphorous; photocatalysis, hydrogen, water-splitting, cocatalyst

TOC content: we report microwave-exfoliated p-type few-layer black phosphorous (BP-nanosheets) as a stable photocatalyst for hydrogen production without any supporting noble metal co-catalyst. We also have elucidated the understanding of the photo-physicochemical reasons that drive this chemistry.

TOC figure: